A Theoretical Study of Alcohol Oxidation by Ferrate

Takehiro Ohta, Takashi Kamachi, Yoshihito Shiota, and Kazunari Yoshizawa*,†

Department of Molecular Engineering, Kyoto University, Sakyo-ku, Kyoto 606-8501, Japan

kazunari@ms.ifoc.kyushu-u.ac.jp

The conversion of methanol to formaldehyde mediated by ferrate (FeO_4^{2-}), monoprotonated ferrate ($HFeO_4^-$), and diprotonated ferrate (H_2FeO_4) is discussed with the hybrid B3LYP density functional theory (DFT) method. Diprotonated ferrate is the best mediator for the activation of the O–H and C–H bonds of methanol via two entrance reaction channels: (1) an addition–elimination mechanism that involves coordination of methanol to diprotonated ferrate; (2) a direct abstraction mechanism that involves H atom abstraction from the O–H or C–H bond of methanol. Within the framework of the polarizable continuum model (PCM), the energetic profiles of these reaction mechanisms in aqueous solution are calculated and investigated. In the addition–elimination mechanism, the O–H and C–H bonds of ligating methanol are cleaved by an oxo or hydroxo ligand, and therefore the way to the formation of formaldehyde is branched into four reaction pathways. The most favorable reaction pathway in the addition–elimination mechanism is initiated by an O–H cleavage via a four-centered transition state that leads to intermediate containing an Fe–O bond, followed by a C–H cleavage via a five-centered transition state to lead to formaldehyde complex. In the direct abstraction mechanism, the oxidation reaction can be initiated by a direct H atom abstraction from either the O–H or C–H bond, and it is branched into three pathways for the formation of formaldehyde. The most favorable reaction pathway in the direct abstraction mechanism is initiated by C–H activation that leads to organometallic intermediate containing an Fe–C bond, followed by a concerted H atom transfer from the OH group of methanol to an oxo ligand of ferrate. The first steps in both mechanisms are all competitive in energy, but due to the significant energetical stability of the organometallic intermediate, the most likely initial reaction in methanol oxidation by ferrate is the direct C–H bond cleavage.

Introduction

High-valent transition metal oxides such as manganese dioxide (MnO_2), potassium permanganate ($KMnO_4$), chromium trioxide (CrO_3), potassium chromate (K_2CrO_4), and potassium dichromate ($K_2Cr_2O_7$) are frequently used for oxidation of organic compounds in laboratory and in industry.[1] However, in addition to their lack in selectivity and difficulty in controlling the experimental conditions, these reagents are corrosive and violently toxic to human beings and to the environment. In view of ever compelling environmental constraints, it is unacceptable for industrial wastes to contain such highly toxic transition metal complexes.[2] Ferrate (FeO_4^{2-}), derived from mineral salts such as the potassium (K_2FeO_4) and barium ($BaFeO_4$) forms, can mediate oxidation of a wide variety of organic compounds such as alcohols,[3,4] amines,[4] hydrazines,[5a] peroxides,[6] hydrocarbons,[7] and thiosulfates[5b] with excel-

lent selectivity. Primary and secondary alcohols are successfully converted into aldehydes and ketones, respectively, but tertiary alcohols are not oxidized.[3] Due to its friendliness to the environment, special interests are directed to the catalytic functions of ferrate.[7] From an X-ray analysis, the crystal structure of FeO_4^{2-} is slightly distorted from T_d symmetry.[8] An isotope labeling experiment of oxygen[6] and IR spectroscopy[9] demonstrated that its mononuclear structure is kept in aqueous solution. Ferrate salt once dried is stable in air, while in water the stability is limited depending on the temperature and pH of solution.[10] For instance, in acidic and neutral media ferrate is reduced by water to evolve O_2, while it is considerably stable in strongly alkaline solution around pH = 10.[11] Since the reaction rate of alcohol oxidation by ferrate is dependent on the pH of solvent, proton or hydroxide is considered to play an important role in the alcohol oxidation.[12–14] In an acidic media, ferrate is protonated and its oxidation ability is greatly increased.

In conjunction with the chemical and biochemical importance for the activation of O–H and C–H bonds

---

* To whom correspondence should be addressed.
† Present address: Institute for Fundamental Research of Organic Chemistry, Kyushu University, Fukuoka 812-8581, Japan.

(1) (a) *Oxidation in Organic Chemistry*; Wiberg, K. B., Ed.; Academic Press: New York, 1965; Part A. (b) *Oxidation in Organic Chemistry*; Trakanovsky, W. S., Ed.; Academic Press: New York, 1973; Part B. (c) *Comprehensive Organic Synthesis (Oxidation)*; Trost, B. M., Ed.; Pergamon: New York, 1991; Vol. 7.
(2) Spiro, T. G.; Stigliani, W. M. *Chemistry of the Environment*; Prentice Hall: New Jersey, 1996.
(3) Audette, R. J.; Quail, J. W.; Smith, P. J. *Tetrahedron Lett.* **1971,** 279.
(4) Tsuda, Y.; Nakajima, S. *Chem. Lett.* **1978,** 1397.
(5) (a) Johnson, M. D.; Hornstein, B. J. *Inorg. Chim. Acta* **1994,** *225,* 145. (b) Johnson, M. D.; Read, J. F. *Inorg. Chem.* **1996,** *35,* 6795.

(6) Goff, H.; Murmann, R. K. *J. Am. Chem. Soc.* **1971,** *93,* 6058.
(7) Delaude, L.; Laszlo, P. *J. Org. Chem.* **1996,** *61,* 6360.
(8) Hoppe, M. L.; Schlemper, E. O.; Murmann, R. K. *Acta Crystallogr.* **1982,** *B38,* 2237.
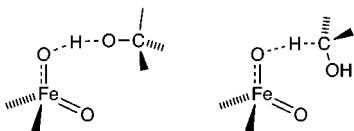(9) Griffith, W. P. *J. Chem. Soc A* **1966,** 1467.
(10) Wagner, W. F.; Gump, J. R.; Hart, E. N. *Anal. Chem.* **1952,** *24,* 1497.
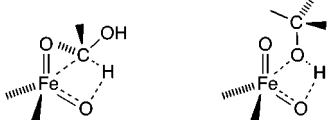(11) Wood, R. H. *J. Am. Chem. Soc.* **1958,** *80,* 2038.
(12) Cyr, J. E.; Bielski, B. H. J. *Free Radical Biol. Med.* **1991,** *11,* 157.
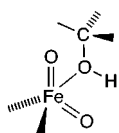
Chart 1

(A) Direct abstraction

(B) [2 + 2] addition

(C) Addition-elimination

by high-valent transition metal-oxides, the widespread use of ferrate in the functionalization of O−H and C−H bonds has spurred considerable interests in the underlying activation mechanism. Previous quantum chemical studies[15−17] of alcohol oxidation by various high-valent transition-metal oxides lead us to believe that alcohol oxidation by ferrate should be initiated by possible entrance reaction channels indicated in Chart 1. In the initial stages of the reaction pathways, (A) shows a direct H atom abstraction from the O−H or C−H bond, (B) shows [2 + 2] addition between the O−H or C−H bond and the Fe−O moiety of ferrate, and (C) shows an addition of methanol to ferrate through the formation of an Fe−O$_{methanol}$ bond. The term "addition−elimination" means that the oxidation is initiated by the addition of alcohol and completed by the elimination of aldehyde from final product complex. At first sight, the [2 + 2] addition mechanism looks similar to the addition−elimination mechanism, but these mechanisms should be strictly distinguished in that the formations of the Fe−C (or O) bond and the FeO−H bond take place in a synchronous concerted manner in the [2 + 2] addition mechanism while the coordination of alcohol and the subsequent formation of the FeO−H bond occur in a stepwise manner in the addition−elimination mechanism. Experimental outputs based on kinetic analyses may be insufficient to determine which mechanism is energetically most favorable among them.

Under such circumstances, theoretical calculations are useful to obtain detailed information about the oxidation processes. Early pioneering theoretical studies of alcohol oxidation by oxo-metal compounds were performed by

Goddard et al.,[15] who applied the generalized valence bond (GVB) method to the oxidation of alcohol, alkane, and alkene by chromyl chloride (CrO$_2$Cl$_2$) and molybdenyl chloride (MoO$_2$Cl$_2$). Ziegler et al.[16] have extensively studied the activation of the C−H and O−H bonds of methanol by a series of d^0 transition metal oxides MO$_2$X$_2$, where M = V, Nb, Ta, Cr, Mo, W, Mn, Tc, Re, Fe, Ru, and Os; X = Cl, from a thermodynamic point of view by using the Amsterdam density functional (ADF) method.[16a,b] Recently they reported detailed reaction pathways of methanol oxidation by MO$_2$X$_2$, where M = Cr, Mo, X = Cl; M = Ru, X = O, from density-functional-theory (DFT) calculations and intrinsic reaction coordinate (IRC) analyses.[16c] To our knowledge, however, no theoretical analysis of alcohol oxidation by ferrate has been performed, probably due to the difficulty in modeling the actual active oxidant. In this article, we present possible mechanisms for the methanol−formaldehyde conversion by ferrate and protonated ferrates.

Computational Details

1. Method of Calculation. We used the hybrid B3LYP DFT method[18] implemented with the Gaussian 98 program.[19] This method consists of the Slater exchange, the Hartree−Fock exchange, the exchange functional of Becke,[18a,b] the correlation functional of Lee, Yang, and Parr (LYP),[18c] and the correlation functional of Vosko, Wilk, and Nusair. The contribution of each energy to the B3LYP energy expression was fitted by Becke on a reference set of molecules.[18b] The B3LYP method has been reported to provide excellent descriptions of various reaction profiles, particularly in geometries, hearts of reaction, barrier heights, and molecular vibrations. For the Fe atom the (14s9p5d) primitive set of Wachters' all electron basis set[20] added by one polarization f-function ($\alpha = 1.05$)[21] resulting in a (611111111|51111|311|1) [9s5p3d1f] contraction was used, and for the other atoms the 6-311G** basis set of Pople and co-workers[22] was used. Vibrational frequencies were systematically computed for all stationary points obtained in order to confirm that each optimized geometry corresponds to a local minimum that has no imaginary frequency or to a saddle point that has only one imaginary frequency. Zero-point-energy corrections were taken into account for calculating the energetics of the reaction pathways.

Our calculations were performed in two steps. After optimizing the geometries of intermediates and transition states at the B3LYP/6-311G** level of theory, the effect of the polarized surrounding of water on the reaction species was evaluated. The dielectric effect of water solvent at 25 °C (ϵ = 78.39) was obtained using the polarized continuum model (PCM)[23] implemented in the Gaussian 98 program. Barone and co-workers[23c] reported a new definition of cavities for calculating solvation free energies by the PCM. The new definition of cavities can be referred to as the united atom model for the

(13) (a) Lee, D. G.; Gai, H. *Can. J. Chem.* **1993**, *71*, 1394. (b) Norcross, B. E.; Lewis, W. C.; Gai, H.; Noureldin, N. A.; Lee, D. G. *Can. J. Chem.* **1997**, *75*, 129.

(14) Audette, R. J.; Quail, J. W.; Smith, P. J. *J. Chem. Soc., Chem. Commun.* **1972**, 38.

(15) (a) Rappé, A. K.; Goddard, W. A., III. *Nature (London)* **1980**, *285*, 311. (b) Rappé, A. K.; Goddard, W. A., III. *J. Am. Chem. Soc.* **1980**, *102*, 5114. (c) Rappé, A. K.; Goddard, W. A., III. *J. Am. Chem. Soc.* **1982**, *104*, 448. (d) Rappé, A. K.; Goddard, W. A., III. *J. Am. Chem. Soc.* **1982**, *104*, 3287.

(16) (a) Ziegler, T.; Li, J. *Organometallics* **1995**, *14*, 214. (b) Deng, L.; Ziegler, T. *Organometallics* **1996**, *15*, 3011. (c) Deng, L.; Ziegler, T. *Organometallics* **1997**, *16*, 716.

(17) Cundari, T. R.; Drago, R. S. *Inorg. Chem.* **1990**, *29*, 3904.

(18) (a) Becke, A. D. *Phys. Rev. A* **1988**, *38*, 3098. (b) Becke, A. D. *J. Chem. Phys.* **1993**, *98*, 5648. (c) Lee, C.; Yang, W.; Parr, R. G. *Phys. Rev. B* **1988**, *37*, 785.

(19) Frisch, M. J.; Trucks, G. W.; Schlegel, H. B.; Scuseria, G. E.; Robb, M. A.; Cheeseman, J. R.; Zakrzewski, V. G.; Montgomery, J. A.; Stratmann, R. E.; Burant, J. C.; Dapprich, S.; Millam, J. M.; Daniels, A. D.; Kudin, K. N.; Strain, M. C.; Farkas, O.; Tomasi, J.; Barone, V.; Cossi, M.; Cammi, R.; Mennucci, B.; Pomelli, C.; Adamo, C.; Clifford, S.; Ochterski, J.; Petersson, G. A.; Ayala, P. Y.; Cui, Q.; Morokuma, K.; Malick, D. K.; Rabuck, A. D.; Raghavachari, K.; Foresman, J. B.; Cioslowski, J.; Ortiz, J. V.; Stefanov, B. B.; Liu, G.; Liashenko, A.; Piskorz, P.; Komaromi, I.; Gomperts, R.; Martin, R. L.; Fox, D. J.; Keith, T.; Al-Laham, M. A.; Peng, C. Y.; Nanayakkara, A.; Gonzalez, C.; Challacombe, M.; Gill, P. M. W.; Johnson, B. G.; Chen, W.; Wong, M. W.; Andres, J. L.; Head-Gordon, M.; Replogle, E. S.; Pople, J. A. *Gaussian 98*; Gaussian Inc.: Pittsburgh, PA, 1998.

(20) Wachters, A. J. H. *J. Chem. Phys.* **1970**, *52*, 1033.

(21) Raghavachari, K.; Trucks, G. W. *J. Chem. Phys.* **1989**, *91*, 1062.

(22) Raghavachari, K.; Binkley, J. S.; Seegar, R.; Pople, J. A. *J. Chem. Phys.* **1980**, *72*, 650.
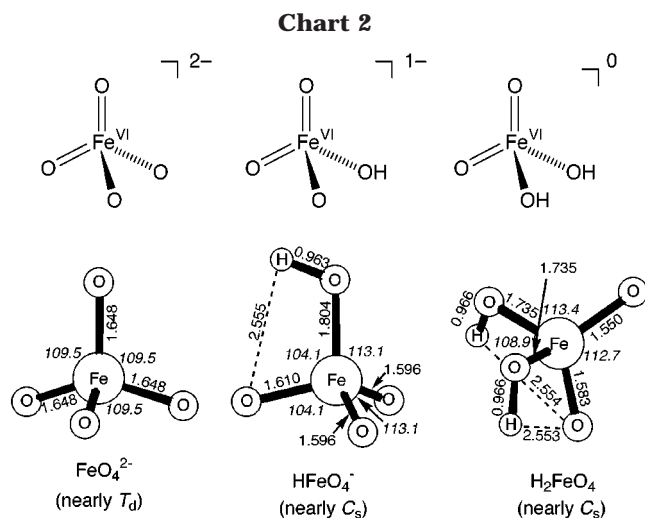
Chart 2

Figure 1. Optimized geometry of ferrate and protonated ferrates. Bond distances in Å and angles (italic) in deg.

Table 1. Spin Densities (spin), Charges (Q), and Energy Levels of the LUMO (eV) of Ferrate and Protonated Ferrates

	FeO_4^{2-}	$HFeO_4^-$	H_2FeO_4
$Q(Fe)$	1.55	1.53	1.55
spin(Fe)	1.50	1.27	1.26
$Q(O_{oxo})^a$	−0.89	−0.68	−0.47
spin(O_{oxo})^a	0.12	0.25	0.35^c
$Q(O_{hydoroxo})^a$		−0.49	−0.31
spin($O_{hydoroxo}$)^a		−0.03	0.02
LUMO (eV)^b	0.01284	0.00315	−0.00619
	(0.01259)	(0.00315)	(−0.00603)

^{a} Average value. ^{b} α Spin−orbital (β spin−orbital). ^{c} Spin densities of two oxo ligands are 0.54 and 0.15.

Hartree−Fock method (UAHF). In their study, the geometries of molecules were optimized in vacuo at the Hartree−Fock level and in some cases reoptimized the structures in water using the PCM-UAHF, in which they found that the effect of solvent on the molecular geometries can be safely neglected when calculating the solvation free energies. We thus think that our computational procedures can reasonably model methanol oxidation by ferrate in water.

2. Ferrate Models. As mentioned above, protonated ferrates are reasonably considered to exhibit stronger oxidation ability.[12,13] We thus built ferrate FeO_4^{2-} and protonated ferrates $HFeO_4^-$ and H_2FeO_4 for our theoretical analyses, as shown in Chart 2. The formal charge of the iron atom is +6. The spin state of these ferrates was set to be a triplet according to magnetic susceptibility measurements of the FeO_4^{2-} salts.[24]

Methanol was chosen as the substrate alcohol. Our efforts were first directed to locate the four-centered transition state for the [2 + 2] addition on the potential energy surface. The direct abstraction mechanism was investigated by making efforts to compute the transition state with a linear O−H−O(OH)$_{ligand}$ array. The addition−elimination mechanism was approached by optimizing the geometry of methanol-coordinating reactant complex.

Results

1. Structures of Ferrate and Protonated Ferrates. Optimized geometries of ferrate and protonated ferrates are shown in Figure 1. No symmetry was imposed in the geometry optimizations; FeO_4^{2-} is nearly T_d and $HFeO_4^-$ and H_2FeO_4 are nearly C_s. Calculated Fe−O$_{oxo}$ distances of 1.65 Å and O−Fe−O bond angles of 109.5° for FeO_4^{2-} are in excellent agreement with an X-ray determined structure of K_2FeO_4 (Fe−O, 1.65 ± 0.01 Å; O−Fe−O, 109.5°).[8] Thus, the B3LYP/6-311G** geometry optimizations are reliable for these systems.

The Fe−O$_{oxo}$ bonds of ferrate are significantly increased in length upon protonation, whereas unprotonated Fe−O$_{oxo}$ bonds are decreased in length. This tendency is more significant in H_2FeO_4 than in $HFeO_4^-$. We show in Table 1 computed atomic charges and spin densities from

Mulliken population analyses and LUMO energies of ferrate and the protonated ferrates. We found an interesting computational result on the spin density distribution in these ferrates. Despite the short Fe−O$_{oxo}$ bonds in the protonated ferrates, $HFeO_4^-$ and H_2FeO_4 have larger spin densities on the oxo ligands than FeO_4^{2-}, which is fully consistent with the experimental findings that protonated ferrate has stronger oxidation ability.[12,13] Since the hydroxo ligands of the protonated ferrates are not a spin carrier, the hydroxo ligands are not expected to mediate direct H atom abstraction, as seen later in this paper. The energy level of the LUMO of ferrate is lowered upon protonation, which suggests that the oxidation ability of the protonated ferrates should be enhanced because of the increased electron accepting ability. Judging from these electronic features, diprotonated ferrate is likely to be the strongest oxidant among these ferrates.

2. Reaction Pathways for the Conversion of Methanol to Formaldehyde by Ferrates. Let us next detail calculated reaction pathways for the methanol−formaldehyde conversion by the ferrates. To elucidate the mechanism of methanol oxidation by these ferrates, we tried to find the transition states of [2 + 2] addition and of direct H atom abstraction and to optimize the geometry of methanol-coordinating reactant complex. However, B3LYP/6-311G* geometry optimizations did not yield these transition states and methanol-coordinating reactant complex for FeO_4^{2-} and $HFeO_4^-$ despite our best efforts, which leads us to conclude that FeO_4^{2-} and $HFeO_4^-$ are not effective for methanol oxidation.[25] On the other hand, H_2FeO_4 was found to mediate methanol oxidation via two entrance channels indicated in Chart 1. One mechanism is initiated by the formation of a methanol-coordinating complex that involves an Fe−O$_{methanol}$ bond. We found the coordination of methanol to H_2FeO_4 and the subsequent breaking of the O−H bond. We term it "addition−elimination mechanism" in that the reaction mechanism includes the addition of methanol to H_2FeO_4 and the elimination of formaldehyde from product (formaldehyde) complex. The other mechanism involves direct H atom abstraction from the O−H or C−H bonds of methanol. We term this "direct abstraction mechanism". We could not obtain the transition state for [2 + 2] addition between the O−H or C−H bond of methanol and the Fe−O moiety of ferrate, and therefore

(23) (a) Miertus, S.; Scrocco, E.; Tomasi, J. *Chem. Phys.* **1981**, *55*, 117. (b) Miertus, S.; Tomasi, J. *J. Chem. Phys.* **1982**, *65*, 239. (c) Barone, V.; Cossi, M.; Tomasi, J. *J. Chem. Phys.* **1997**, *107*, 3210. (d) Cossi, M.; Barone, V.; Cammi, R.; Tomasi, J. *Chem. Phys. Lett.* **1996**, *225*, 327.
(24) (a) Hrostowski, H. J.; Scott, A. B. *J. Chem. Phys.* **1950**, *18*, 105. (b) Audette, R. J.; Quail, J. W. *Inorg. Chem.* **1972**, *11*, 1904.

(25) Geometry optimizations of reactant complexes, intermediates, and transition states were performed in vacuo and after that single-point energy calculations were carried out by including the polarization effect of water with the PCM. Thus, there is a possibility that under the solvation conditions, FeO_4^{2-} and $HFeO_4^-$ may form a reactant complex or a transition state for the activation of the O−H and C−H bond of methanol. However, the inclusion of solvation effect on geometry optimizations for this system is probably small.
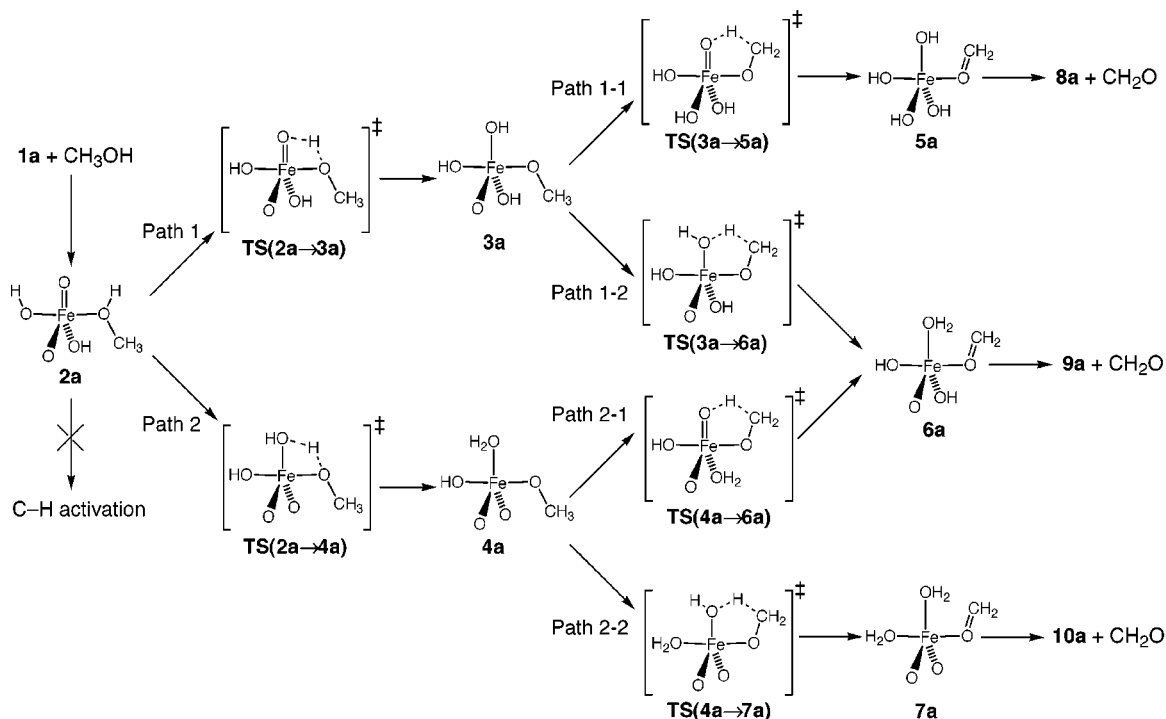
Figure 2. Pathways for the methanol−formaldehyde conversion by diprotonated ferrate in the addition−elimination mechanism.

the [2 + 2] addition mechanism in Chart 1 is unlikely to occur from our calculations. We will describe the addition−elimination mechanism in section 2.1 and the direct abstraction mechanism in section 2.2 from energetic, structural, and electronic points of view.

2.1. Addition−Elimination Mechanism. 2.1.1. Reaction Paths. Let us first look at the profile of the addition−elimination mechanism shown in Figure 2. We named diprotonated ferrate **1a** for the discussion below. This reaction mechanism begins with the coordination of methanol to **1a**. Path 1 involves the O−H activation by an oxo ligand via **TS(2a→3a)** in the initial stage to yield **3a** which has resultant methoxo, oxo, and hydroxo ligands, while in Path 2 the O−H bond is activated by a hydroxo ligand via **TS(2a→4a)** in the initial stage to yield **4a** which has resultant methoxo, oxo, hydroxo, and water ligands. The transition vector on **TS(2a→3a)** and **TS(2a→4a)** is predominantly located on the migrating hydrogen atom, and therefore these do not correspond to the transition states for the [2 + 2] addition mechanism. We could not find a five-centered transition state for the C−H bond dissociation while keeping the Fe−O$_{methanol}$ bond in **2a**; thus, the initial step in the addition−elimination mechanism is not likely the C−H bond activation.

The formation of methoxide-coordinating intermediates **3a** and **4a** is followed by the activation of a C−H bond via Path 1-1, 1-2, 2-1, and 2-2. Path 1-1 involves the C−H bond activation by the other oxo ligand via **TS(3a→5a)** to lead to formaldehyde-coordinating complex **5a**, while in Path 1-2 the C−H bond activation is mediated by a hydroxo ligand to yield **6a** via **TS(3a→6a)**. A C−H bond of the methoxo ligand in **4a** is activated in Path 2-1 and 2-2 by an oxo and hydroxo ligand to yield product complexes **6a** and **7a**, respectively. By releasing formaldehyde from product complexes **5a**, **6a**, and **7a**, diprotonated ferrate completes the conversion of methanol to formaldehyde.

Table 2. Relative Energies, Imaginary Frequencies of Transition Vectors, and $\langle S^2 \rangle$ Values of the Reaction Species Involved in the Addition−Elimination Mechanism

	$E_{\text{solv}}{}^a$	$E_{\text{vac}}{}^a$	iω^b	$\langle S^2 \rangle^c$
1a + methanol	0^d	0^e		2.001^f
2a	−6.7	−10.7		2.001
3a	1.7	−2.9		2.001
4a	−6.2	−11.4		2.001
5a	−59.5	−61.9		2.001
6a	−53.1	−53.2		2.000
7a	−31.0	−34.0		2.001
8a + CH$_2$O	−50.4	−49.2		2.001^f
9a + CH$_2$O	−43.8	−43.0		2.001^f
10a + CH$_2$O	−21.1	−18.2		2.001^f
TS(2a→3a)	19.8	10.1	1517	2.002
TS(2a→4a)	14.4	6.7	974	2.001
TS(3a→5a)	13.8	4.6	924	2.178
TS(3a→6a)	12.2	3.9	1231	2.000
TS(4a→6a)	4.2	−2.1	1551	2.001
TS(4a→7a)	10.8	4.4	1115	2.072

^{a} Relative to the energy of **1a** + methanol (units in kcal/mol). ^{b} Imaginary frequencies of transition vectors (units in cm^{-1}). ^{c} The expectation value of S^2 operator. ^{d} Absolute value of −1681.468398 hartree. ^{e} Absolute value of −1681.584112 hartree. ^{f} For **1a**, **8a**, **9a**, and **10a**, respectively.

2.1.2. Energy Diagrams. We show in Figure 3 computed potential energy diagrams for the methanol−formaldehyde conversion along the addition−elimination mechanism. Solvent effects are included in the energies with the aid of the PCM.[23] In Table 2, we list computed relative energies in solvent and in vacuo, imaginary frequencies of transition vectors, and expectation values of the S^2 operator of the reaction species involved in this mechanism.

The binding energy of methanol in **1a** was computed to be 6.7 kcal/mol in water solution and 10.7 kcal/mol in vacuo, being larger than those obtained in CrO$_2$Cl$_2$ (0.8 kcal/mol), MoO$_2$Cl$_2$ (3.9 kcal/mol), and RuO$_4$ (0.5 kcal/mol).[16] We conclude in view of Table 2 that these
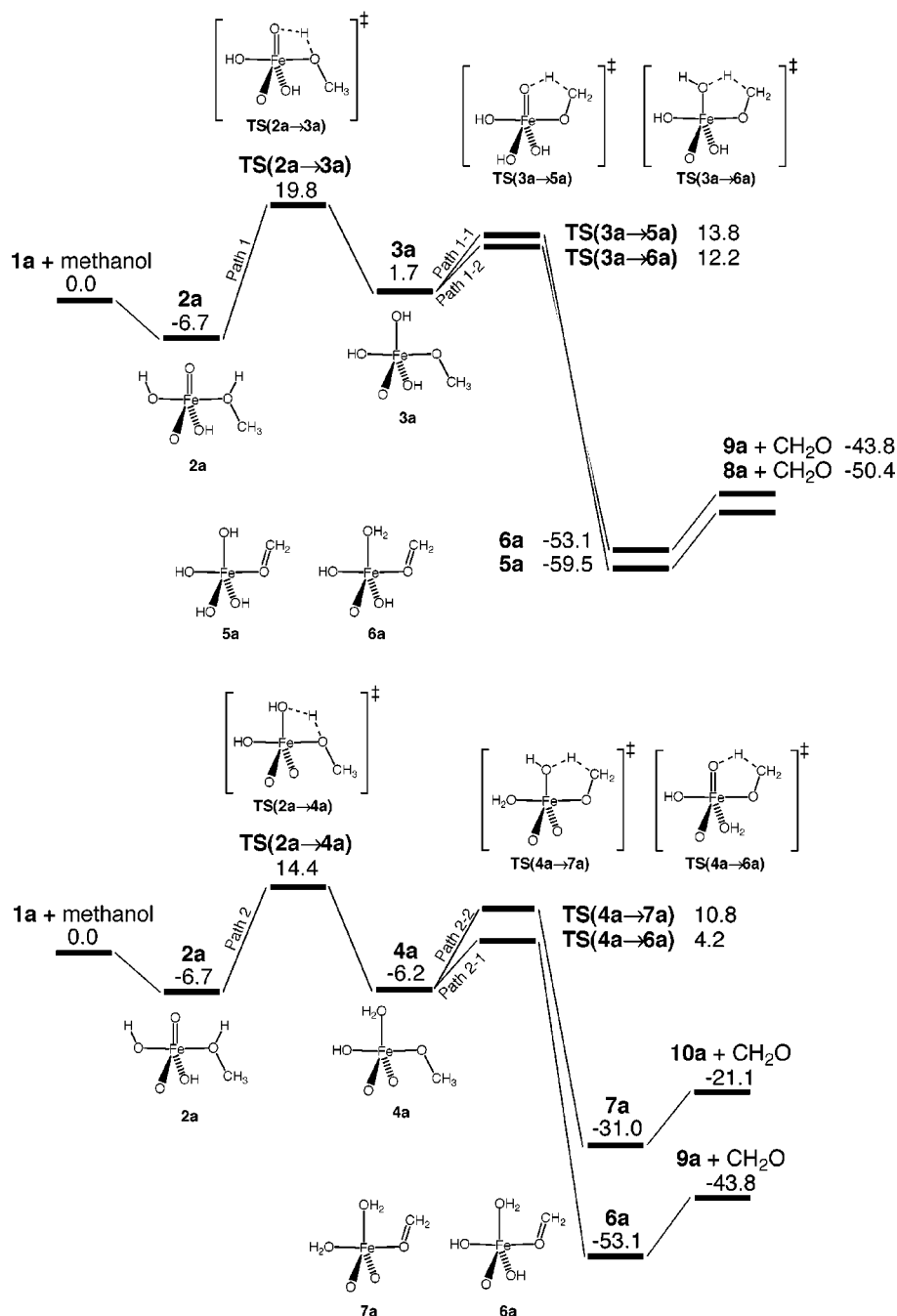
Figure 3. Potential energy diagrams along the addition—elimination mechanism in water (units in kcal/mol).

energetic profiles in this addition—elimination mechanism are not significantly changed in solvent and in vacuo. Computed $\langle S^2 \rangle$ values of about 2 are fully consistent with those expected for triplet molecules, and thus our calculations adequately describe the triplet state of ferrate. The activation energy from **2a** to **TS(2a→3a)** is 26.5 kcal/mol and that to **TS(2a→4a)** is 21.1 kcal/mol, suggesting that the hydroxo ligand can dissociate the O—H bond with a smaller activation energy than the oxo ligand. We further performed calculations of the energies of **TS(2a→3a)** and **TS(2a→4a)** with various DFT methods. Computed energies in Table S1 of Supporting Information demonstrate that the energy difference between **TS(2a→3a)** and **TS(2a→4a)** in vacuo is 3.4 kcal/mol at B3LYP, 3.1 kcal/mol at B3PW91, 2.1 kcal/mol at BLYP, 0.1 kcal/mol at BP86, and 0.1 kcal/mol at

PW91PW91; the hybrid methods, which give better results in general, lead **TS(2a→4a)** to lie in energy below **TS(2a→3a)**. Thus, our B3LYLP calculations should correctly describe the energetics of the TSs that are involved in the alcohol oxidation by ferrate.

The activation energies for the C—H bond dissociation via **TS(3a→5a)** in Path 1-1 and **TS(3a→6a)** in Path 1-2 are 12.1 and 10.5 kcal/mol, respectively. The C—H activation via **TS(4a→6a)** in Path 2-1 and that via **TS(4a→7a)** in Path 2-2 requires 10.4 and 17.0 kcal/mol, respectively, thus suggesting that the C—H activation is preferred by the oxo ligand. Judging from these energetic profiles, the hydroxo ligand is also an important activator of the C—H and O—H bonds of methanol in the addition—elimination mechanism. The entire reaction profile along Path 2-1 is 43.8 kcal/mol exothermic, and thus the
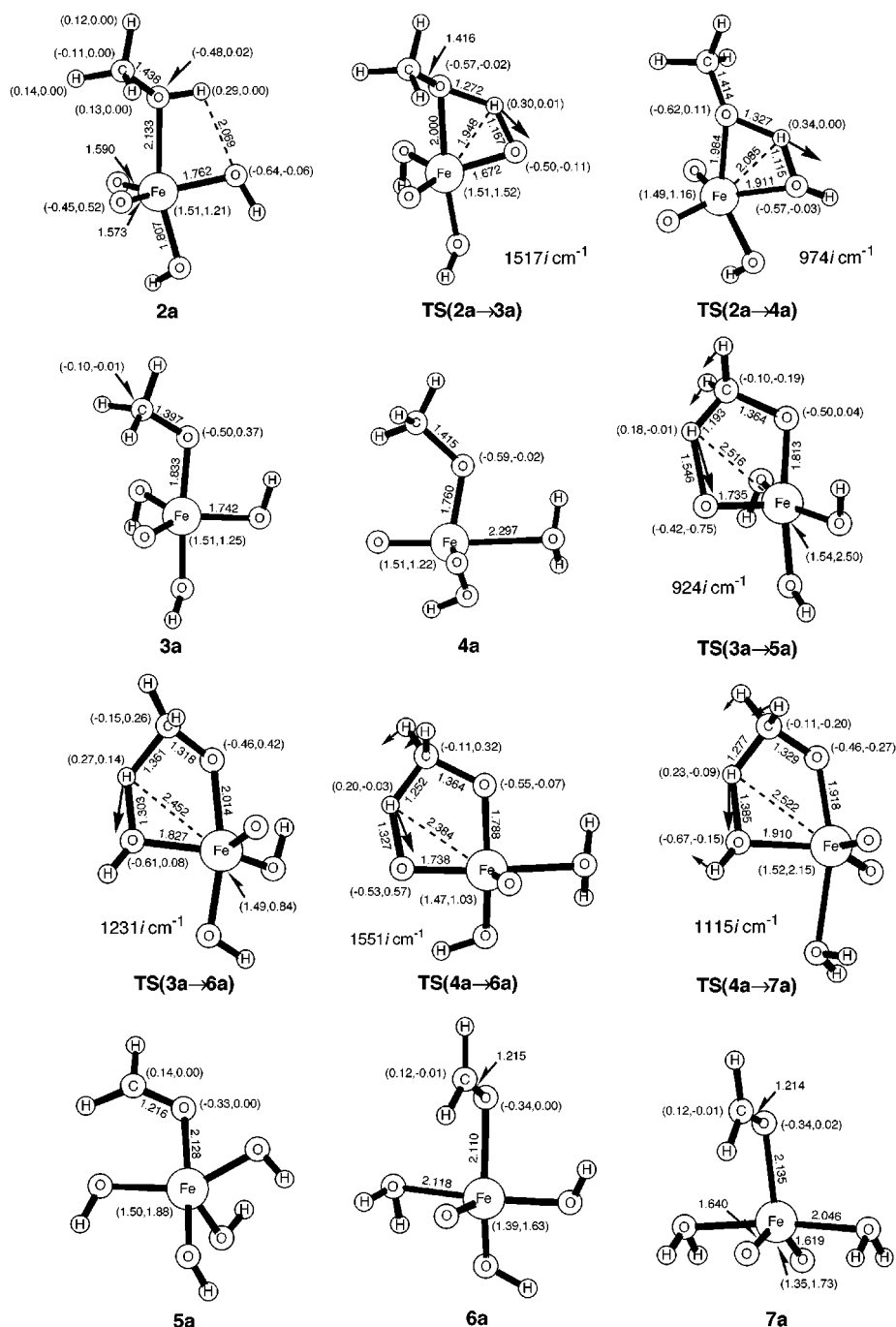
Figure 4. Optimized geometry, charges, and spin densities (charge, spin density) of intermediates and transition states in the addition−elimination mechanism. Bond distances in Å. Imaginary modes of vibration which characterize the transition states are indicated.

conversion of methanol to formaldehyde is energetically preferred and all the reaction pathways are reasonably considered to take place in view of the energetic profiles shown in Figure 3. The most likely reaction pathway is Path 2-1.

2.1.3. Optimized Geometries. We show in Figure 4 optimized geometries of the intermediates and transition states involved in the addition−elimination mechanism. Bond distances are indicated in units of Å. Atomic charges and spin densities are indicated in parentheses in this order, and transition vectors and corresponding imaginary frequencies of the transition states are also indicated.

Methanol-coordinating complex **2a** has a trigonal-bipyramidal structure with respect to the iron center. The $Fe-O_{methanol}$ bond distance of 2.133 Å is shorter than those reported for the methanol-coordinating adducts of $Cr_2O_2Cl_2(CH_3OH)$ ($Cr-O_{methanol} = 2.898$ Å), MoO_2Cl_2 (CH_3OH) ($Mo-O_{methanol} = 2.317$ Å), and $RuO_4(CH_3OH)$ ($Ru-O_{methanol} = 2.560$ Å).[16] The total charge of methanol in **2a** is +0.1, and thus this small charge transfer from methanol to the iron center can play an important role in the coordination of methanol. Neither FeO_4^{2-} nor $HFeO_4^-$ gave such a methanol adduct, and therefore the lowering of the energy level of the LUMO, by which the LUMO can accept electron density from the HOMO of
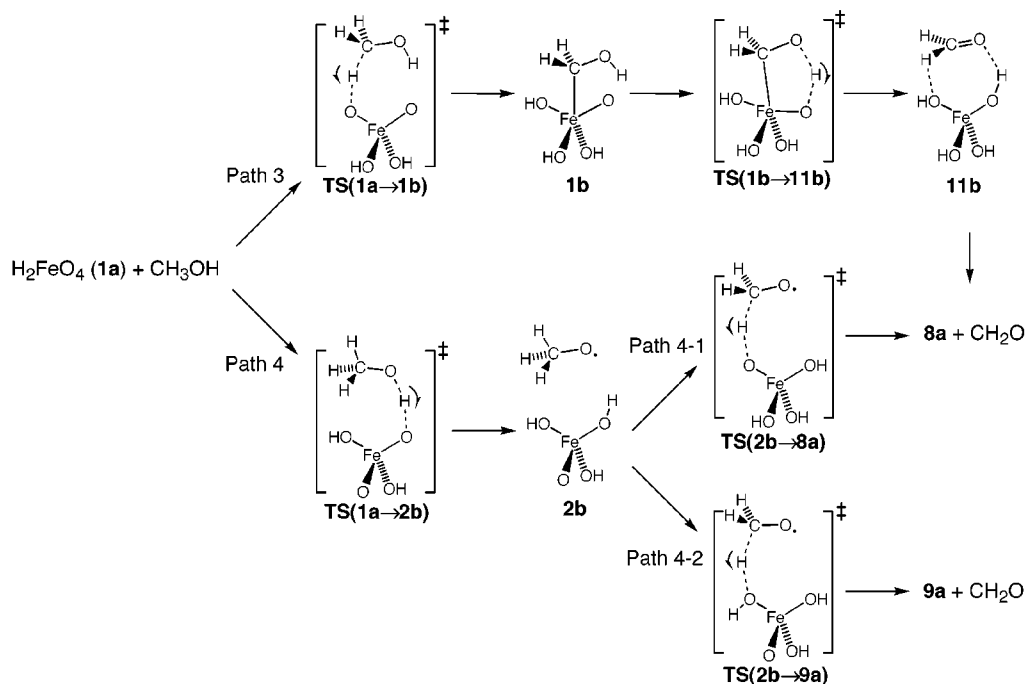
Figure 5. Pathways for the methanol−formaldehyde conversion by diprotonated ferrate in the direct abstraction mechanism.

methanol, should be important for the coordination and activation of methanol in the addition−elimination mechanism.

Transition states **TS(2a→3a)** and **TS(2a→4a)** possess four-centered structures concerning the H atom abstractions. Resultant methoxide coordinating complexes **3a** and **4a** have Fe−O$_{methoxide}$ bonds of 1.833 and 1.760 Å, respectively, **3a** and **4a** taking trigonal-bipyramidal structures. The C−H bond activations via **TS(3a→5a)** (in Path 1-1), **TS(3a→6a)** (in Path 1-2), **TS(4a→6a)** (in Path 2-1), and **TS(4a→7a)** (in Path 2-2) involve five-centered structures. These transition state structures are reasonable for these electronic processes. There are three kinds of final formaldehyde complexes; **7a** lies in energy above **5a** and **6a**.

2.2. Direct Abstraction Mechanism. 2.2.1. Reaction Paths. We show in Figure 5 the profile of the direct abstraction mechanism. Intermediates and transition states which newly appear in the direct abstraction mechanism are labeled **b** with numbers, and the complexes labeled **a** are also involved in the addition−elimination mechanism.

In Path 3, a C−H bond of methanol is initially dissociated via **TS(1a→1b)**, and the resultant carbon radical species would form a complex either by the coordination of the carbon atom (**1b**) or the oxygen atom (**1b′**) of methanol to the iron center, **1b′**, not shown in Figure 5. It is reasonable that a generated radical species is bound to an unsaturated metal active center. However, as will be shown in section 2.2.3, **1b** is rather stable in energy compared with **1b′**, and thus we do not discuss anymore the reaction pathway involving **1b′**. An organometallic intermediate that has an Fe−C bond was proposed by Lee and co-workers[13] to be a key intermediate in the catalytic alcohol oxidation by ferrate. They proposed that the intermediate would be formed by [2 + 2] addition between a C−H bond of alcohol and an Fe−O$_{oxo}$ bond of ferrate. However, no transition state for such concerted [2 + 2] addition was found on the

potential energy surface, as mentioned above. As will be shown in section 2.2.3, the C−H bond is preferentially activated by an oxo ligand in the direct abstraction mechanism, and subsequently the O−H bond of **1b** is cleaved by the oxo ligand in a concerted manner leading to final complex **11b**.

In Path 4, the O−H bond is first cleaved via **TS(1a→2b)** to give rise to **2b**, in which methoxy radical has weak bonding interaction with ferrate. Radical intermediate **2b** is energetically less stable than **1b** and **1b′**, in which substrate radical is strongly bound to the iron active center. A C−H bond of the methoxy radical in **2b** is next activated either by the oxo or hydroxo ligand via **TS(2b→8a)** (in Path 4-1) and **TS(2b→9a)** (in Path 4-2) to yield formaldehyde and complexes **8a** and **9a**. When the methoxy radical in **2b** is trapped by the iron center, subsequent C−H bond activation would proceed along Path 1-1 and 1-2 of the addition−elimination mechanism.

2.2.2. Energy Diagrams. Figure 6 shows computed energy diagrams for the methanol−formaldehyde conversion along the direct abstraction mechanism. Computed activation energies of 13.6 and 17.1 kcal/mol for the first step in Path 3 and Path 4, respectively, are comparable in energy. However, since intermediate **1b** is energetically very stable in comparison with **1b′** and **2b**, C−H bond activation in the first stage would preferentially occur along Path 3 via **1b**. We can rule out the possibility of the other reaction pathways. In Table 3, we list relative energies in water solvent and in vacuo, frequencies of transition vectors, and expectation values of the S^2 operator of the reaction species involved in the direct abstraction mechanism. We see from Table 3 that the energetic profiles in solvent and in vacuo are not remarkably different and the reaction pathway that proceeds through **1b** (Path 3) is clearly the most favorable reaction pathway.

2.2.3. Optimized Geometries. We show in Figure 7 optimized geometries of the reaction intermediates and transition states involved in the direct abstraction mecha-
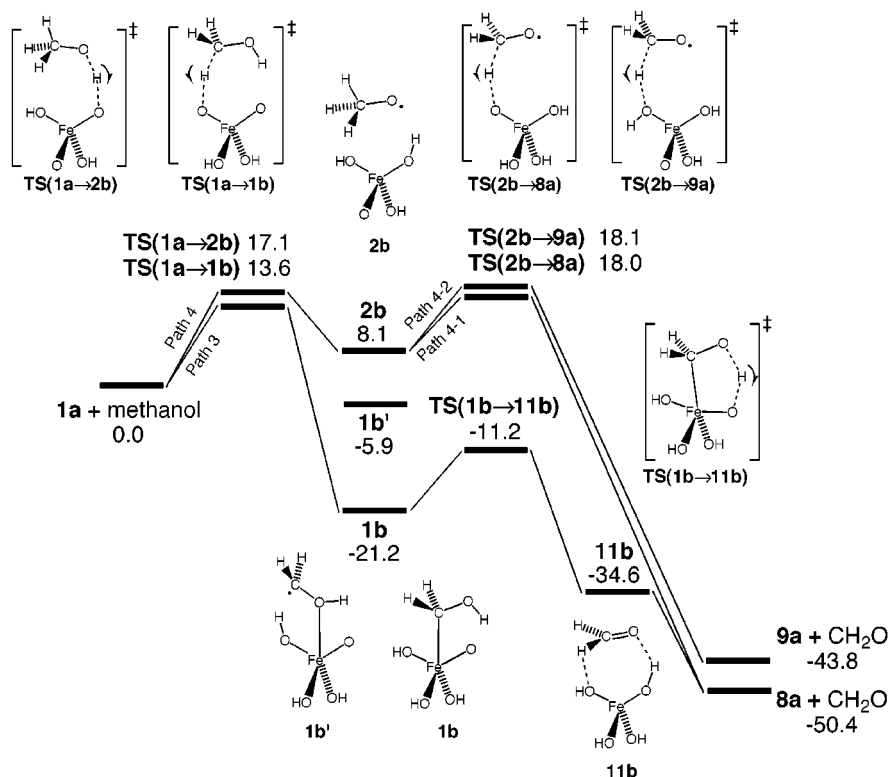
Figure 6. Potential energy diagrams along the direct abstraction mechanism in water (units in kcal/mol).

Table 3. Relative Energies, Imaginary Frequencies of Transition Vectors, and $\langle S^2 \rangle$ of the Reaction Species Involved in the Direct Abstraction Mechanism[a]

	$E_{solv}{}^b$	$E_{vac}{}^b$	$i\omega^c$	$\langle S^2 \rangle^d$
1b	−21.2	−21.1		2.373
1b′	−5.9	−4.9		2.000
2b	8.1	2.5		2.000
11b	−34.6	−43.1		2.076
TS(1a→1b)	13.6	7.3	1280	2.002
TS(1a→2b)	17.1	8.1	1586	2.000
TS(1b→11b)	−11.2	−19.3	703	2.275
TS(2b→8a)	18.0	7.5	1478	2.004
TS(2b→9a)	18.1	10.1	1790	2.003

[a] Intermediate species which are also included in the addition–elimination mechanism in Table 2 are omitted from this table. [b] Relative to the energy of **1a** + methanol in Table 2 (units in kcal/mol). [c] Imaginary frequencies of transition vectors (units in cm^{-1}). [d] The expectation value of S^2 operator.

nism. Let us first look at Path 3. The Fe···O$_{methanol}$ and Fe···C$_{methanol}$ distances in **TS(1a→1b)** are 3.242 and 3.326 Å, respectively, indicating that methanol is not directly coordinating to the iron center. The C–H and H–O$_{oxo}$ distances are 1.277 and 1.296 Å, respectively, which are appropriate for the direct abstraction process. Thus, this direct H atom abstraction is a simple electronic process for the C–H bond dissociation as well as the O–H bond formation. Intermediate **1b** has an Fe–C bond of 2.147 Å. There is a hydrogen bond in this intermediate, as indicated by a dotted line. In **1b′** the carbon atom of substrate is a spin carrier with a spin density of 0.93, and thus the C–H bond dissociation can take place in a homolytic cleavage manner, but this intermediate is not important from a viewpoint of energetics. The O–H bond of substrate in **1b** is activated via five-centered **TS(1b→11b)**, keeping the Fe–C bond length 2.477 Å, and formaldehyde complex **11b** is formed as a consequence.

In Path 4 the O–H bond is initially activated via **TS(1a→2b)** with a linear O–H–O(Fe) array. In intermediate **2b** the methoxy radical interacts weakly with the hydroxo ligand, and while keeping the weak interaction, an H atom is abstracted from a C–H bond by an oxo ligand via **TS(2b→8a)** or by a hydroxo ligand via **TS(2b→9a)** to produce formaldehyde. Path 4 is energetically unfavorable, as seen in Figure 6.

3. Kinetic Isotope Effects. Kinetic isotope effect (KIE) (k_H/k_D) is an important measure in discussing how the electronic process for H atom abstraction of substrate hydrocarbon takes place in catalytic and enzymatic reactions. In this section, we consider the isotope effects in methanol oxidation by diprotonated ferrate in the addition–elimination and the direct abstraction mechanisms. The kinetic isotope effects were obtained by transition state theory[26] with the following expression.[27,28]

$$\frac{k_H}{k_D} = \left(\frac{m_D^R \, m_H^\#}{m_H^R \, m_D^\#} \right)^{3/2} \left(\frac{I_{xD}^R \, I_{yD}^R \, I_{zD}^R}{I_{xH}^R \, I_{yH}^R \, I_{zH}^R} \right)^{1/2} \left(\frac{I_{xH}^\# \, I_{yH}^\# \, I_{zH}^\#}{I_{xD}^\# \, I_{yD}^\# \, I_{zD}^\#} \right)^{1/2} \times$$

$$\frac{q_{vD}^R \, q_{vH}^\#}{q_{vH}^R \, q_{vD}^\#} \exp\left(-\frac{E_H^\# - E_D^\#}{RT} \right)$$

Here m, I, q, and E indicate the molecular mass, the moment of inertia, the vibrational partition function, and the activation energy, respectively. The superscript R specifies the reactant complex **2a** for the addition–elimination mechanism or the substrate for the direct

(26) McQuarrie, D. A. *Statistical Thermodynamics*; University Science Book: Mill Valley, 1973.

(27) Filatov, M.; Shaik, S. *J. Phys. Chem. A* **1998**, *102*, 3835.

(28) Yoshizawa, K.; Kagawa, Y. *J. Phys. Chem. A* **2000**, *104*, 9347. Possible mechanisms for methanol oxidation by the bare FeO$^+$ species are described in this paper.
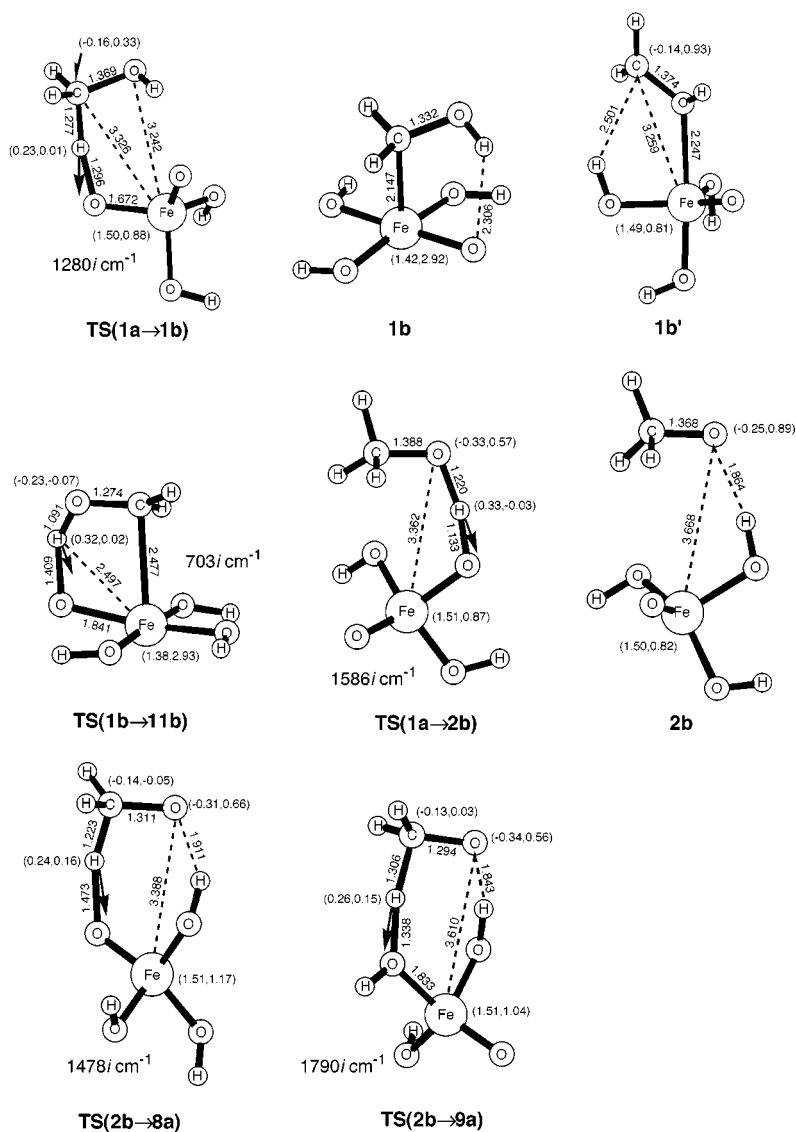
Figure 7. Optimized geometry, charges, and spin densities (charge, spin density) of intermediates and transition states in the direct abstraction mechanism. Bond distances in Å. Imaginary modes of vibration that characterize the transition states are indicated.

Table 4. Kinetic Isotope Effect for the Methanol Oxidation by Diprotonated Ferrate at 298 K

	k_H/k_D
TS(2a→3a)	4.9^a
TS(2a→4a)	4.4^a
TS(1a→2b)	8.2^a
TS(1a→1b)	8.0^b

^{a} For the D-labeled substrate of CH_3OD. ^{b} For the D-labeled substrate CD_3OH.

abstraction mechanism, and the superscript # indicates the transition state. The subscript H means the species including CH_3OH and the subscript D means D-labeled methanol CH_3OD or CD_3OH. The last exponential term is dominant in this equation because the other terms can be almost all canceled between denominators and numerators. The numerators in the last exponential term come from the fact that C–H dissociation has a lower activation energy than C–D dissociation on account of the former's greater zero-point vibrational energy and thermal correction. Table 4 summarizes computed values of k_H/k_D for the concerted O–H cleavage via **TS(2a→3a)**

and **TS(2a→4a)** and the direct C–H and O–H cleavage via **TS(1a→1b)** and **TS(1a→2b)**, respectively.

The concerted O–H activation processes in **TS(2a→3a)** and **TS(2a→4a)** show k_H/k_D values of 4.9 and 4.4, respectively, whereas the direct abstraction process in **TS(1a→2b)** shows a value of 8.2; this direct process affords larger values of k_H/k_D than the concerted processes, as expected.

Discussion

Having described the computed reaction pathways for methanol oxidation by diprotonated ferrate, let us consider which mechanism can better reproduce experimental findings in the light of kinetic studies. While monoprotonated ferrate has been supposed to be an actual oxidant for the oxidation of alcohols, our DFT study predicted that ferrate should be attached by two protons in order to have sufficient oxidizing power for methanol. The protonation of FeO_4^{2-}, which results in increasing the spin density of the oxo ligands as well as lowering the energy level of the LUMO, would strengthen its oxidation ability. In particular, the increased spin density

of the oxo ligands should be important for direct H atom abstractions because the hydroxo ligands with small spin densities are not effective for the direct abstractions. Our recent DFT study on the reactivity of the MO^+ complexes (M = Sc, Ti, V, Cr, Mn, Fe, Co, Ni, and Cu) demonstrates that the reactivity to methane oxidation is proportional to the spin density on the oxo ligand.[29] Besides these effects, a charge effect is important for methanol oxidation by ferrate; i.e., upon diprotonation the total charge of ferrate becomes neutral, and consequently neutral methanol can easily access without electrostatic repulsion. Protonated chromate $(CrO_4{}^{2-})$[30] and manganate $(MnO_4{}^-)$[31] were also proposed to show stronger oxidation ability.

Previous experimental studies suggested that it is possible to distinguish between alcohol oxidation reactions that are initiated by O−H or C−H activation by comparing the oxidation rate of alcohol with that of ether having a structure similar to the alcohol. For example, Westheimer and co-workers[32] demonstrated that chromic acid reacts 1500 times faster with isopropyl alcohol than diisopropyl ether and concluded that the initial reaction between chromic acid and the alcohols involves ether formation. Conversely, when the oxidation is initiated by C−H activation, alcohols and ethers are considered to be oxidized in an equal rate. Lee and co-workers[13a] reported that ferrate reacts with alcohol and THF at similar rates. Because only a ring-opened product was obtained from the oxidation of cyclobutanol by ferrate, a free radical intermediate is considered to be involved in the reaction. Substituted mandelic acid did show insensitivity to substituent effects, and therefore substantial charges are not built up in the transition state. These findings led them to propose that the reaction is initiated by [2 + 2] addition between an Fe−O$_{oxo}$ bond and an α-C−H bond of alcohol to give an organometallic intermediate that is subsequently decomposed by homolytic cleavage of the resulting Fe−C bond.[13a] This is supported by theoretical predictions by Goddard et al.[15] Our DFT calculations also suggest that the C−H bond activation should take place in the initial stage of the reaction to form **1b**. We therefore agree that alcohol should initially be activated in C−H bond to form an organometallic intermediate, but the [2 + 2] mechanism is unlikely in the methanol−formaldehyde conversion by ferrate. We think that the Fe−C bond should be kept during the subsequent O−H bond breaking, and thus the opening of ring substrates observed[13a] would occur during the first C−H activation before trapping by the iron center. This reaction mechanism is in contrast to that of the bare FeO^+ complex, which leads methanol to formaldehyde in the gas phase by means of Fourier transform ion cyclotron resonance (FTICR) mass spectroscopy. In this reaction, O−H activation is proposed as the first step due to the fact that neither the formation of $FeOH^+$ and $CH_2OH\cdot$ radical nor the complementary products CH_2OH^+ and neutral $FeOH^+$ are observed.[33] This gas-phase reaction is similar to Path 2-1 in the addition−elimination mechanism.

Our theoretical KIE analyses will give an answer with respect to the reaction mechanism for the conversion of methanol to formaldehyde. We tried to find experimental data of KIEs for methanol oxidation to compare with theoretical results but we could not. Lee and co-workers investigated KIEs with 2-propanol and mandelic acid as substrate, in which α-C−H bonds were D-labeled, and found that the k_H/k_D values fall in a range of 3−4.[13a] They also investigated KIEs using 2-propanol and substituted ethanols of which the hydroxyl groups were D-labeled.[13b] The k_H/k_D values are 10 for 2-propanol and 5−6 for substituted ethanols. On the other hand, Audette and co-workers investigated KIEs with benzyl alcohols as substrate and found the k_H/k_D values fall in a range of 5−8.[14] Thus, KIEs are significantly dependent on substrates and we cannot directly compare our theoretical results with these experiments. If the direct C−H bond cleavage is really operative in the entrance reaction channel of methanol oxidation by ferrate, an experimental KIE measurement should show a k_H/k_D value of about 8.

Conclusions

We demonstrated in this study that diprotonated ferrate is an effective oxidant for the activation of the C−H and O−H bonds of methanol, which would be ascribed to the increase in the oxo spin density and the lowered energy level of the LUMO. Diprotonated ferrate was found to effectively oxidize methanol to formaldehyde via two reaction mechanisms, the addition−elimination and the direct abstraction mechanisms. In the addition−elimination mechanism, the C−H and O−H bonds of methanol are activated by a concerted H atom migration to an oxo or hydroxo ligand of diprotonated ferrate. In the direct abstraction mechanism, the initial C−H bond dissociation with a linear C−H−O(Fe) transition state is energetically preferred. The first steps for methanol oxidation by diprotonated ferrate in the addition−elimination and the direct abstraction mechanisms are all competitive from a viewpoint of activation energy. Due to the energetical stability of intermediate **1b**, in which generated carbon radical is strongly bound to the iron active center, the methanol-formaldehyde conversion by ferrate could be initiated by the direct C−H activation. We conclude that Path 3 in Figure 5 is energetically most likely. Path 2-1 in the addition−elimination mechanism in Figure 2 is also likely to occur. We finally calculated KIEs in the concerted mechanism and the direct abstraction mechanism using transition state theory. Computed values of k_H/k_D for the concerted O−H activation are 4.6 on average and for the direct O−H and C−H activations are 8.2 and 8.0, respectively, which can be a measure for better understanding the oxidation mechanism of ferrate.

Supporting Information Available: Optimized geometries of **8a**, **9a**, **10a**, and **11b** and Table S1 that summarizes the energetic profiles of **TS(2a→3a)** and **TS(2a→4a)** at various DFT methods. This material is available free of charge via Internet at http://pubs.acs.org.

JO001193B

(29) Shiota, Y.; Yoshizawa, K. *J. Am. Chem. Soc.* **2000**, *122*, 12317.

(30) Westheimer, F. H. *Chem. Rev.* **1949**, *45*, 419.

(31) Lee, D. G.; Chen, T. *J. Am. Chem. Soc.* **1993**, *115*, 11231.

(32) Brownell, R.; Leo, A.; Chang, Y. W.; Westheimer, F. H. *J. Am. Chem. Soc.* **1960**, *82*, 406.

(33) Schröder, D.; Wesendrup, R.; Schalley, C. A.; Zummack, W.; Schwarz, H. *Helv. Chim. Acta* **1996**, *79*, 123.